

THE EFFECTS OF ELECTRON DAMAGE  
ON THE SHEAR MODULUS OF COPPER

---

Douglas Appleby Powell, Jr.

and

Harry Seagrove Sellers

Library  
U. S. Naval Postgraduate School  
Monterey, California









THE EFFECTS OF ELECTRON DAMAGE  
ON THE SHEAR MODULUS OF COPPER

\* \* \* \* \*

Douglas A. Powell, Jr.

and

Harry S. Sellers





THE EFFECTS OF ELECTRON DAMAGE  
ON THE SHEAR MODULUS OF COPPER

by

Douglas Appleby Powell, Jr.  
Commander, United States Navy

and

Harry Seagrove Sellers  
Lieutenant, United States Navy

Submitted in partial fulfillment  
of the requirements  
for the degree of  
MASTER OF SCIENCE  
IN  
PHYSICS

United States Naval Postgraduate School  
Monterey, California

1 9 5 6

Thesis

P 253

This work is accepted as fulfilling  
the thesis requirements for the degree of  
MASTER OF SCIENCE  
IN  
PHYSICS

from the  
United States Naval Postgraduate School



## PREFACE

Since the turn of the century, the physical sciences have made vast strides in the atomic and nuclear fields. The Rutherford scattering formula solidified the nuclear hypothesis and led to its acceptance. Early experiments dealt primarily with nuclear reactions; known projectile particles were used to produce radiation which was studied by means of emission, absorption and scattering. Attention was concentrated on the information derived from such measurements with little or no attention being paid to the damage which was done to the structure of the material.

The development of the chain-reaction pile, and the recent improvements in accelerators, have made it imperative to understand the effects such powerful sources of radiation have upon the fuel and structural materials involved. It is known that uranium fuel expands in the process of fissioning in a chain-reaction pile and it is reasonable to expect that the physical properties in other elements are affected by irradiation.

The structural elements in a bulk material are composed of definite lattice arrangements of atoms which will be disordered in some manner by incident particles. Since the war, studies have been carried out to learn the basic mechanisms involved in the damage to crystal lattices, how such damage may repair itself, and what effect these imperfections have upon the physical and mechanical properties of the bulk material.



The investigation reported here was conducted in the first half of 1956 at the United States Naval Postgraduate School. It has as its aim the study of the dependency of the shear modulus of copper upon electron irradiation, and attempts to arrive at some conclusions concerning the mechanisms involved.

The authors wish to express their appreciation for the assistance, cooperation, and encouragement given them by Professor E. C. Crittenden, to whom credit for the initial concept of the experiment should be given, and Professor E. A. Milne, whose knowledge of and experience with particle accelerators made the project possible. They also wish to acknowledge the valuable technical assistance given them by Mr. M. K. Andrews, Mr. K. C. Smith and Chief Opticalman R. C. Moeller, U. S. Navy.





## TABLE OF CONTENTS

Item	Title	Page
CHAPTER I	INTRODUCTION . . . . .	1
	1. Previous Work	
	2. Concept of Experiment	
	3. Factors in Radiation Damage by Electrons	
	4. Factors in Annealing of Radiation Damage	
CHAPTER II	EQUIPMENT. . . . .	7
	1. General Considerations	
	2. Basic Equipment	
	3. Cooling System	
	4. Target Assembly	
	5. Temperature Control	
	6. Counting System	
CHAPTER III	SPECIMEN . . . . .	16
	1. History	
	2. Preparation	
CHAPTER IV	EXPERIMENTAL PROCEDURE . . . . .	19
	1. Preparation Phase	
	2. Irradiation Phase	
	3. Annealing Phase	
CHAPTER V	EXPERIMENTAL RESULTS . . . . .	23
CHAPTER VI	DISCUSSION . . . . .	27
CHAPTER VII	CONCLUSIONS . . . . .	31
BIBLIOGRAPHY	. . . . .	32
ILLUSTRATIONS AND GRAPHS	. . . . .	33



# LIST OF ILLUSTRATIONS

Figure		Page
1.	General Arrangement of Equipment . . . . .	33
2.	Deflection, Target, and Cooling Systems . . . . .	34
3.	"Vacuum side" of Inner Surface of Annular Cross-sectioned Vacuum Tank . . . . .	35
4.	Recess and Fittings for Aluminum Window . . . . .	36
5.	Liquid Nitrogen Reservoir . . . . .	37
6.	Target Assembly . . . . .	38
7.	Lower Portion of Target Assembly . . . . .	39
8.	Heater in Lowered Position for Pulse Anneals of Specimen . . . . .	40
9.	Torsion Pendulum . . . . .	41
10.	Preparation and Handling Equipment for Specimen . .	42
11.	Ozalids Exposed by Electron Beam of Window and Specimen . . . . .	43
12.	Current Through Window vs Deflection Voltage . . . .	44
13.	Shear Modulus vs Integrated Electron Flux, Specimen No. 1 . . . . .	45
14.	Shear Modulus vs Integrated Electron Flux, Specimen No. 2 . . . . .	46
15.	Shear Modulus vs Integrated Electron Flux, Trial Specimen . . . . .	47
16.	Shear Modulus vs 15 Minute Pulse Anneal Temperature, Specimen No. 1 . . . . .	48
17.	Shear Modulus vs 15 Minute Pulse Anneal Temperature, Specimen No. 2 . . . . .	49
18.	15 Minute Pulse Anneals of Undamaged Specimen . . .	50



# TABLE OF SYMBOLS AND ABBREVIATIONS

(Listed in the order of their use in the text)

$E_0$	- Threshold energy for displacement of an atom from its lattice site
f.c.c.	- Face centered cubic crystal
$\Gamma$	- Orientation function of shear modulus in a crystal plane
G	- Shear modulus
$S_{44}, S_{11}, S_{12}$	- Elastic coefficients of metal crystals
$\alpha, \beta, \gamma$	- Direction cosines for orientation function vector
I	- The moment of inertia of the torsion pendulum
$\ell$	- Length of copper specimen wire
$\tau$	- Resonant period of torsion pendulum
r	- Radius of specimen wire



# CHAPTER I

## INTRODUCTION

### 1. Previous Work

During the last five years, more and more investigators have been turning their attention to questions concerning the nature of radiation damage in crystalline solids. As of October 1955, J. W. Glenn<sup>(7)</sup> had tabulated nearly 150 known experiments concerned with the effects of all types of radiation on many materials, as observed through changes in almost every conceivable physical property. Radiations used have included electromagnetic radiation, alpha particles, electrons, protons, neutrons, deuterons, and heavier ions. Bombarded materials have included both metals and non-metals in elementary form and as alloys and compounds. The properties observed have been equally diversified, however resistivity in metals has been a favorite because of ease of measurement and control of experimental variables.

Although seemingly comprehensive when combined with the theoretical work that has been done concurrently, this array of information still represents only a small start toward answering the many questions concerned with the nature and mechanism of radiation damage.

Notably meager in the realm of experimental evidence are two types of information, namely the effects of irradiation on the elastic constants such as Young's modulus and shear





modulus; and effects on any properties in general, of bombardment by electrons - presumed to create only point defects, the simplest type of damage. That this is a reasonable assumption can be shown by consideration of the mean free path of the electron, and of the energy and momentum conservation principles of inelastic collisions between an electron and a nucleus.

Four previous experiments have measured the elastic constants. Two, concerned with austenitic steel and copper under neutron bombardment at pile temperatures showed no change. Work by Dieckamp and Crittenden,<sup>(3)</sup> however, indicated a decrease of the shear modulus of copper on irradiation with 20 Mev deuterons with one third recovery on annealing at  $-125^{\circ}\text{C}$  and the other two thirds recovery between  $-50^{\circ}\text{C}$  and  $+100^{\circ}\text{C}$ .

Dieckamp<sup>(4)</sup> did bombard copper with one Mev electrons but was unable to obtain a pre-irradiation measurement of the shear modulus. He reported the following changes in shear modulus with thermal annealing:  $-196^{\circ}\text{C}$  to  $-50^{\circ}\text{C}$ , 4% increase;  $-25^{\circ}\text{C}$  to  $+50^{\circ}\text{C}$ , no change;  $+75^{\circ}\text{C}$ ,  $\frac{1}{2}\%$  decrease;  $100^{\circ}\text{C}$  to  $200^{\circ}\text{C}$ , no change;  $250^{\circ}\text{C}$  to  $350^{\circ}\text{C}$ , 2% decrease.

## 2. Concept of Experiment

In order to supplement these data in a conclusive manner an experiment was decided upon wherein the change in shear modulus was to be measured as a function of electron bombardment and also as a function of thermal annealing subsequent to bombardment. Since previous work indicated that this type of damage might be unstable at room temperature, it was determined to perform the bombardment at as low a temperature as practicable,



namely liquid nitrogen temperature,  $-195.8^{\circ}\text{C}$ . The availability of the horizontal two Mev Van de Graaff Electrostatic Accelerator at the Naval Postgraduate School was to be exploited by building the necessary equipment to irradiate and measure the sample in place without any transfer or handling, thus eliminating the possibility of cold work or uncontrolled temperature rises obscuring the radiation effects.

Copper was chosen as the substance to be irradiated. The shear modulus was to be measured by observation of the period of a torsion pendulum using, as the torsional element, the sample in the form of a pure copper wire .010 inches in diameter and approximately  $1\frac{1}{4}$  inches long. The advantages of these choices will be brought out in Chapter Three.

### 3. Factors in Radiation Damage by Electrons

Many models and concepts have been proposed to explain the changes observed with radiation damage. The following paragraphs present in random fashion some of the basic ideas which may apply to this investigation, and which have gained fairly general acceptance.

Consider a face centered cubic metal, such as copper, being bombarded by a beam of energetic electrons. An incoming electron when reacting with an atom in the crystal lattice can collide elastically either with an orbital electron or with the nucleus. In the former case there should be no observable changes in the properties of the metal as the orbital electron receiving the energy can easily lose its energy and return to its original state. However in the case of the nucleus inter-



action it is conceivable that if the energy transfer were great enough the nucleus could be knocked out of its lattice site and pass between its nearest neighbors into an interstitial position. There would be associated with this movement a threshold energy,  $E_0$ , necessary to get the atom initially past its nearest neighbors. This energy has been determined experimentally by Eggen and Laubenstein<sup>(6)</sup> to be about 25 ev for f.c.c. metals bombarded with electrons. How far the interstitial would be removed from its original lattice site - now a vacancy - would depend on the amount of energy in excess of  $E_0$  which the atom received.

Further disposition of these point defects could include migration to dislocations or crystal boundaries, recombination and annihilation, or clustering into groups of point defects. The rates at which these processes occur would be a function primarily of the subsequent thermal energy imparted to the crystalline structure, however they should also be affected by such things as density and initial separation of the interstitial/vacancy pairs, impurities, and density of other defects in the lattice such as edge and screw dislocations.

It should further be noted that although electrons produce damage at a much slower rate, they have two distinct advantages over heavier particles. First, they can reasonably be considered to produce homogeneously distributed damage throughout the specimen, and second, the damage should be of the simplest type, free from the thermal spikes accompanying high energy transfers associated with the heavy particles. These ad-



vantages are due both to the greater penetrating power of the electron and the fact that any one particle can probably produce only one interstitial/vacancy pair as previously noted.

G. J. Dienes<sup>(5)</sup> has calculated from the atomic interaction potentials and on the basis of the number of bonds made and broken, the change in the elastic coefficients due to the presence of one percent interstitials and vacancies. Using these values he has computed the change in the shear modulus of copper to be an increase of 6.3% due to one percent interstitials and a decrease of 1.5% due to one percent vacancies. Thus a net increase in shear modulus should be displayed by copper on bombardment with electrons if formation of these point defects is the only process going on.

#### 4. Factors in Annealing of Radiation Damage

The observation of the recovery as a function of temperature, following radiation damage gives insight into the kinetics of the processes involved. By observing the recovery of a property with time at one temperature and comparing with similar data at a second temperature it is possible, by means of the familiar chemical rate equations, to determine activation energies for the recovery process involved in the temperature range observed. This experiment did not attempt to obtain the isothermal annealing curves necessary for this type of analysis, but did set out to locate temperature zones of increased recovery activity in order to correlate with previous annealing work by other investigators.

Many mechanisms for recovery have been proposed on the





basis of both theory and experimental results, but there is as yet no overwhelming evidence in favor of any one mechanism. In fact it is fairly apparent that the processes vary among the different temperature zones and further, within some zones the overall result seems to be the sum of several processes. This is to be expected on consideration of the many possibilities involved.

Among the more frequently proposed processes of recovery are the independent migration at different activation energies of vacancies and interstitials and the annihilation of close pairs. In particular there is fairly good agreement among experimenters in attributing an activation energy of 1.2 ev, found on annealing copper in the vicinity of 100°C, to vacancy migration. Interstitial migration is generally conceded to occur at lower temperatures.

In addition to the simple effect due to the loss from the crystal of these point defects there is the possibility that they may migrate to dislocations. This would cause portions of the dislocation to climb forming notches in the line. Although the notches might have a low resistance to motion along the dislocation, the undisturbed portions of the dislocation would have increased resistance to motion in the slip plane. That is, glide in the slip plane would be restricted by the pinning action of the vacancies and interstitials thus causing an increase in shear modulus. This will be considered in greater detail in Chapter Six.



## CHAPTER II

### EQUIPMENT

#### 1. General Considerations

The main consideration in the design of the equipment was the utilization of the horizontal Van de Graaff electrostatic accelerator located at the United States Naval Postgraduate School. The unrestricted availability of this accelerator made it possible to test the equipment as constructed and to keep it in place as a temporary addition to the accelerator system. The equipment could be tailored to fit, and refinements made, as the work progressed.

The equipment was so designed that the investigation of the dependency of the shear modulus of copper upon electron irradiation could be carried out as one continuous operation. The specimen, once placed in the assembly, could be irradiated, pulse annealed and measured without being transferred at any time. In this manner the uncertainties of induced plastic deformation were reduced to a minimum.

The Van de Graaff Electrostatic Accelerator employed was a Type A, Model H/S, HVI-34, built and installed by High Voltage Engineering Corporation. It is capable of supplying a 150 microampere beam at two million volts energy.

#### 2. Basic Equipment

Figures 1 and 2 show the overall arrangement of the equipment in its relation to the accelerator and accessory apparatus.



The accelerator tube extension conducts the electron beam from the Van de Graaff to the target space. The deflection coil is used to vertically deflect the beam and distribute it approximately uniformly over the length of the specimen. The target assembly container is a large brass tank of annular cross section, Figure 1 (see also Figure 12 for diagram of cross section), the center portion of which is the target space and is at atmospheric pressure. The annular section is integral with the Van de Graaff vacuum system through the accelerator tube extension (drift tube). The vacuum provides a thermal barrier between room temperature and the liquid nitrogen temperature maintained in the target space. A small window of .003 inch aluminum, Figures 3 and 4, separates the vacuum system from the target space and allows the electron beam to pass through to the specimen.

The deflection coil power supply was controlled by a variac. Referring to Figure 12, the curve is the plot of the total beam current received through the window as measured by the circuit shown. Sufficient deflection voltage was used so that the specimen was irradiated only by the reasonably linear central portion of the beam's vertical sweep. The deflection used resulted in a uniform flux of  $5.8 \times 10^{13}$  electrons-cm<sup>-2</sup>-sec<sup>-1</sup> at the window. The specimen was located about one and a quarter inches beyond the window.

Due to the deflection of the electron beam, a considerable amount of heat was produced in the vicinity of the window which made it difficult to control the temperature rise of the speci-



men. This was countered by inserting a one-inch thick block of aluminum in the drift tube about six inches ahead of the window. The block contained a slot cut to match the window. This block intercepted the unused portion of the beam and the secondaries produced within the drift tube, allowing only those with the proper direction to pass through. The heat generated by these undesirable electrons was thus dissipated to the surrounding atmosphere via the accelerator tube extension which was cooled by a blower.

The aluminum window fitting was inserted as an integral part of the inner surface of the vacuum tank, Figure 3. A slotted copper shield was placed within the vacuum space, external to the recessed window, acting to further mask off the unused portion of the electron beam and to dissipate heat as far away from the window as possible. The window was recessed in order to shorten window to specimen distance thereby reducing dispersion. Optimum alignment in the beam of the several slots, window specimen and thermocouple was accomplished by means of ozalid "shadow pictures", Figure 11, exposed by the electron beam.

The window, Figure 4, consisted of a double thickness of 1.5 mil aluminum foil held in place by means of a lead pressure-distributing ring and a brass hold-down plate. It was found that such an arrangement using normal length steel screws resulted in an excellent vacuum seal at room temperature, but that vacuum leaks occurred at liquid nitrogen temperature ( $-195.8^{\circ}\text{C}$ ). To counter this, it was necessary to devise a differential





expansion system which would draw the hold-down plate tighter at low temperatures. This was accomplished by using 3/4-inch length steel bushings under the heads of brass hold-down screws. This system held a vacuum equally well at room temperature and at the low temperature at which the equipment was operated.

The target space was maintained at liquid nitrogen temperature by means of a second annular cross-sectioned tank serving as a liquid nitrogen reservoir, Figure 5. This tank did not completely line the inside of the target space since design considerations required that a slot be left in order for the tank to fit over the window protrusion. The slot was made full length to facilitate manufacture, although it would have contributed to better cooling of the window area if liquid nitrogen had been in direct contact with the window recess. As designed, however, it worked satisfactorily. The two stainless steel one-half inch O. D. tubes shown were for the purpose of filling the tank and for venting. The small 3/16 copper tubing located between the filling and venting tubes was for cooling gaseous helium, to be described below.

By lining the target space with liquid nitrogen, it was possible to maintain the entire lower portion of this space at or near  $-195^{\circ}\text{C}$ . This feature was designed into the equipment in order to "freeze in" electron damage by reducing the thermal annealing effects, a procedure recommended by Cooper and Mills<sup>(1)</sup> and used by others.



An interesting digression is the fact that when testing a tank for leaks with liquid nitrogen it was found advisable to do so in an oxygen-free space. The oxygen condensed fast enough to obscure nitrogen leaks or to give the impression that there were leaks when in reality the tank was tight.

### 3. Cooling System

The liquid nitrogen tank provided for the general maintenance of the target space at  $-195^{\circ}\text{C}$ , but in order to supply positive cooling of the specimen both during irradiation and during the annealing phase of a run it was necessary to have a flow of gas over the specimen - preferably a gas at  $-195^{\circ}\text{C}$ . At this temperature the choice lay between using nitrogen or helium. It would have been possible to vent the liquid nitrogen tank, described above, through the cooling system rather than to atmosphere. Externally supplied helium, however, was chosen due to its better heat transfer characteristics which resulted in more efficient cooling of the specimen for a given flow of gas. This choice also allowed better control of the cooling flow, it being found desirable to restrict or discontinue it completely while measurements were being taken.

The helium gas was initially cooled to liquid nitrogen temperature by passing it through a pre-cooler, Figures 1 and 2, which consisted of a copper moisture trap and a coil of some twenty feet of copper 1/4-inch O. D. tubing contained in a dewar flask filled with liquid nitrogen and located alongside the brass target tank. From the pre-cooler, the helium was sent to the target space, undergoing a final cooling in the internal



nitrogen reservoir before being directed up around the specimen by means of a concentric annular orifice, Figure 7. During bombardment a flow of about three liters per minute was sufficient to keep the temperature rise of the specimen below 20°. Following a pulse anneal of the specimen, the helium flow was directed up through the furnace, Figure 8, and served to speed the process of cooling the system back down to liquid nitrogen temperature for the taking of data.

The upper six inches of the walls of the target space were manufactured from 10 mil stainless steel, rather than brass, to serve as a thermal barrier between outer room temperature and the liquid nitrogen temperature. This thermal barrier reduced liquid nitrogen usage.

#### 4. Target Assembly

An overall view of the target assembly is shown in Figure 6 with a closeup of the specimen and torsion pendulum shown in Figure 7. The target assembly was suspended from a plexiglass cover plate by means of three one-quarter inch rods. The upper portion of the supporting rods was stainless steel tubing, coinciding with the thermal barrier discussed above. The furnace slides on the front two rods with the back rod used for a strengthening and as a wiring and piping support. This target assembly occupied the center of the target space.

The plexiglass cover not only provided support for the specimen, torsion pendulum and heater, but also provided the means for sealing the target space against moisture. It was necessary to prevent moisture from entering the target space



since condensation would affect the period of the pendulum and also fog the optical system used to measure the period. The cover, when sealed as completely as possible, still did not provide an adequate moisture barrier over long periods. It was found necessary to use the cooling helium flow for the secondary purpose of maintaining the target space in a helium atmosphere slightly above atmospheric pressure. This prevented contamination of the target space by moisture.

The specimen was suspended from the central independent rod, as can be seen in Figures 6 and 7. Included in the target assembly were provisions for externally adjusting the specimen and pendulum with respect to height and angular position. Figure 9 shows the torsion pendulum with the specimen acting as the torsion element. Schmid and Boas<sup>(11)</sup> give a value of 0.10 kilograms per square millimeter as the critical shear stress of pure copper for the (111) plane. Taking into consideration the fact that in a f.c.c. slip occurs along the face of the tetrahedron formed by the possible (111) planes and in the [110] direction, it was found that a weight of 18.6 grams could be tolerated. The pendulum and mounting rod together weighed 17.3 grams. Visual examination and measurement of the specimen following a data run were indecisive in detecting any slip. From the results obtained by the pulse annealing of an undamaged specimen, Figure 18, slip is considered unlikely to have occurred.

A stub bar magnet inserted through the shank of the pendulum, and at right angles to its axis, provided the means of initiating oscillations externally.





The view in Figure 7 of the specimen and of the thermocouple used during bombardment is that seen by the cathode rays.

The furnace, shown in the annealing position in Figure 8, was a 25 watt, ceramic resistor. It was so mounted that it could be lowered or raised without disturbing the specimen. The upper cross piece holding the furnace in line was hollow and opened into a stainless steel tube which extended up through the plexiglass, providing a means of externally positioning the furnace. Upon completion of a pulse anneal this tube was uncorked and a strong flow of helium exhausted through the furnace to speed the cooling-down process. A variac was used to control the voltage applied to the furnace, with a thermocouple attached to the inside of the furnace for temperature readings.

#### 5. Temperature Control

Temperatures within the target space were taken by means of two thermocouples. One thermocouple was located as shown in Figure 7 about one inch beyond the specimen and in the clear with respect to shielding by the specimen during irradiation. This provided for the control of the temperature rise of the specimen during bombardment. The coverage of the specimen and thermocouple by the cathode rays is shown in Figure 11. The second thermocouple was fastened inside the furnace, and provided the means of controlling the anneal temperatures.

The thermocouples were iron-constantan with the fixed or "cold junction" at 0°C. The temperature - E.M.F. values used were those obtained from a standard calibration table<sup>(8)</sup> cor-



rected for local conditions. A Rubicon potentiometer was employed to measure the E.M.F.

The accuracy of the thermocouples in measuring the temperature of the specimen was ascertained by temporarily substituting a third thermocouple in place of the specimen. An optimum helium flow was also determined. On this basis the temperature of the specimen was maintained below  $-175^{\circ}\text{C}$  during bombardment. The furnace temperature was accurate to within  $\pm 2^{\circ}\text{C}$ .

## 6. Counting System

The motion of the torsion pendulum was observed by means of a beam of light focused upon the concave mirror mounted on the pendulum, Figure 9. The 45 degree mirror noted in Figure 7 served the dual purpose of directing the vertical light beam onto the concave mirror as well as passing it back out along the same path onto a centimeter scale. A reticle in the lamp provided a hairline for accurately determining the oscillations. A Hewlett-Packard Electronic Counter, Model 522B, was employed as the crystal controlled timer. The period of the oscillation was obtained from averaging the time for 100 periods. The accuracy of this visual method of period determination is considered to be five parts in ten thousand.



## CHAPTER III

### SPECIMEN

#### 1. History

Copper is well known and has been used extensively in previous determinations of the effects of irradiation upon the physical and mechanical properties of crystals. The choice of copper thus provides a means of correlation between this and similar investigations.

The copper specimens used in this investigation had a reasonably well known history. These were 99.999% pure Johnson-Matthey copper bar which had been rolled down first from one-quarter inch to 3/32 inch by passing the bar between a pair of grooved rollers. This process produced a "flashing" on either side of the wire which was trimmed off. The specimen was then die drawn to 10 mil and annealed in a vacuum for fifteen minutes at 950°C. This anneal resulted in an average [322] direction fiber orientation parallel to the axis of the wire and in a grain size approximating the wire diameter. The fiber orientation had been verified by x-ray diffraction.

The desirable fiber orientation would be  $[11\bar{1}]$ , since the shear modulus in the (111) plane has an orientation function,  $\Gamma$ , which is constant. This means that the shear modulus is independent of direction in the (111) plane. The (322) plane is within  $11^\circ$  of the (111) plane, thus the shear modulus in the (322) plane should be nearly isotropic.



In any given direction, the shear modulus for a f.c.c. is

$$\frac{1}{G} = S_{44} + 4\Gamma \left[ (S_{11} - S_{12}) - \frac{1}{2} S_{44} \right] \quad (10) \quad \Gamma = \alpha^2\beta^2 + \beta^2\gamma^2 + \gamma^2\alpha^2$$

where  $\alpha, \beta, \gamma$  are the direction cosines of this orientation vector. From Schmidt and Boas<sup>(12)</sup>  $S_{11} = 15 \times 10^{-13}$ ;  $S_{12} = -6.3 \times 10^{-13}$ ; and  $S_{44} = 13.3 \times 10^{-13} \text{ cm}^2\text{-dyne}^{-1}$ .

As mentioned above, the orientation function for the (111) plane is constant with a value of 0.250. The orientation function in the (322) plane is nearly constant, with a mean value of 0.239. From these, mean theoretical values for G are determined to be  $3.59 \times 10^{11}$  and  $3.66 \times 10^{11} \text{ dynes-cm}^{-2}$ . The mean value of the shear modulus in the (322) plane is thus seen to be a very good approximation to that in the (111) plane. From this discussion it is considered that the values of relative shear modulus obtained in the course of this investigation are valid.

## 2. Preparation

Figure 10 shows the preparation jig used for attaching the specimen to the mounting rods. The tips of the mounting rods were cleaned and coated with a drop of silver solder. The wire specimen was carefully cut to length, about one and a quarter inches long, while being held in the ceramic protective tube. One mounting rod was then heated just in back of the solder and one end of the specimen inserted when the solder was molten. With the ceramic tube withdrawn, the second mounting rod was heated and touched to the free end of the sample by sliding it in the groove under the clamp. Care was taken not to bend or





distort the sample during this process. While the sample and mounting rods were cooling down from soldering temperatures, one jig clamp was left loose to allow for contractions without imposing a strain on the wire. Warm water and a camel hair brush were used to clean the flux from the specimen. This resulted in a specimen which was relatively free of flux, however some surface oxides were still present. None of the specimens were etched.

After preparation, the specimen was inspected visually under a binocular microscope and then measured by means of a microscope comparator. The length of the specimen was taken to be that part of the wire between the solder wetted surfaces. Uncertainties in the effective length of the specimen were introduced in this manner as it was difficult to determine where the solder ceased to wet the copper, however the uncertainties would only become important if absolute shear modulus was desired.



## CHAPTER IV

### EXPERIMENTAL PROCEDURE

#### 1. Preparation Phase

After preparation of the specimen in the mounting rods it was maintained with a minimum of cold work either in the preparation jig or assembly yoke, Figure 10. The specimen was transferred to the target assembly by means of the assembly yoke which was not removed until the target assembly was being lowered into place. From this point on, the pendulum was mainly supported by the damping magnet, Figure 7, which also eliminated oscillation of the pendulum until specimen and pendulum were raised clear of it by adjusting nuts, Figure 6.

After the target assembly was positioned the target space was scavenged of all air with a stream of helium gas and sealed up as well as possible. From then on the target space was maintained in helium at a pressure slightly above atmospheric pressure by a supply of precooled helium gas via the specimen cooling system. Normal leakage of the helium gas out of the target space provided for an adequate cooling flow over the specimen.

The next step was to lower the specimen heating coil and anneal the specimen for 15 minutes at a temperature of 300°C. This served to put the specimen in a "base" condition with respect to the subsequent annealing process so that any removable lattice defects not associated with the radiation damage would



be removed prior to commencement of the run. Following this preliminary anneal the heater was raised and the specimen was brought to liquid nitrogen temperature and an initial period measurement taken.

The period of a torsional pendulum is related to the shear modulus of the torsional element by:

$$G = \frac{8\pi I \ell}{\tau^2 r^2}$$

where G is the shear modulus; I, the moment of inertia of the pendulum;  $\ell$  and r the length and radius of the element; and  $\tau$  the period. The measurements of the period were always accomplished by timing 100 oscillations of the pendulum. It was found that the timing of 100 oscillations was reproducible, after practice, to within .05 seconds simply by observing the hair-line in the focused light beam from the pendulum mirror as it traversed a graduated scale and manually starting and stopping the crystal timer.

The actual oscillatory motion of the pendulum was held to the very minimum to avoid cold work. A two cm. initial peak to peak swing of the light beam on the scale was sufficient for accuracy and this corresponded to less than 10 minutes of arc displacement of the pendulum from equilibrium. This in turn resulted in a maximum shear stress in the average specimen of not over  $7 \times 10^6$  dynes/cm<sup>2</sup>. Schmid and Boas<sup>(11)</sup>, list the critical shear stress of 99.9% pure copper as 0.10 kg/mm<sup>2</sup> or  $9.80 \times 10^6$  dynes/cm<sup>2</sup>, thus the elastic limit should not have been exceeded.

That it was not being exceeded was experimentally verified at the conclusion of a run by intentionally attempting to deform



the specimen with excess oscillatory amplitude. It was found that an amplitude of three to four times that used in the measurement process did not measurably alter the period.

After the first anneal and measurement, the specimen was allowed to stand in a static condition for eight to ten hours and the period was measured every two to three hours to further observe if any changes not attributable to the irradiation were taking place. No significant change was observed.

## 2. Irradiation Phase

Once these preliminaries were completed the irradiation process was commenced. It was found advisable to stop every 30 minutes to replenish liquid nitrogen in the reservoir around the specimen in order to insure that its temperature was maintained as low as possible. Of the 260 watts in the beam, probably 100 watts of heat was being disposed of by the liquid nitrogen.

The amount of irradiation given to a sample was limited usually by the time available to the investigators. It required about 24 hours to expose the specimen to an integrated flux of  $2.7 \times 10^{18}$  electrons/cm<sup>2</sup> exclusive of the 15 to 20 hours preparation and preliminaries. Data runs, once commenced, were carried to completion without interruption over a 60 hour period.

## 3. Anneal Phase

Following the irradiation period the heating coil was lowered around the specimen and a systematic pulse annealing procedure was commenced wherein  $\tau$  was measured at liquid nitrogen temperature following each 15 minutes anneal at successively increasing





temperatures from  $-175^{\circ}\text{C}$  to  $+300^{\circ}\text{C}$  in increments of  $25^{\circ}$ . (One specimen was carried to  $+400^{\circ}\text{C}$ ). On each pulse anneal the specimen was heated and cooled as quickly as possible, however, it took on the order of one minute to reach  $300^{\circ}\text{C}$  from liquid nitrogen temperature and probably 15 minutes to return coil and specimen to less than  $-190^{\circ}\text{C}$ . The dependence of  $\tau$  on temperature was experimentally determined to be such that variations in  $\tau$  due to a five degree temperature spread were well within the precision of the measurement.

It should once again be emphasized that everything was designed to eliminate the possibility of plastic deformation as a variable. The specimen was not removed or handled from the time it was in place for bombardment until after the annealing phase had been completed.



## CHAPTER V

### EXPERIMENTAL RESULTS

The results of the irradiation phase and annealing phase for each of two specimens (numbers one and two) together with the irradiation phase of a trial specimen and a control "annealing phase" on an unirradiated specimen, are shown in Figures 13 through 18. Each circled point on the graph is the average of from two to six successive measurements by the procedure outlined in Chapter IV. The vertical line through the points indicates the maximum spread of individual measurements and not a standard deviation. Since more measurements were taken when a larger spread was found, it is felt that all points are about equally valid.

Relative shear modulus, i.e.  $\frac{I\ell}{\tau^2}$  in gm-cm<sup>3</sup>/sec<sup>2</sup>, is plotted as the ordinate on all graphs. The absolute shear modulus can be computed by multiplying by the constant  $\frac{8\pi}{\lambda^4}$  where  $r$  is the radius of the specimen or .005 inches in this experiment. However the absolute modulus would have no particular meaning and therefor was not shown. It might be of interest to state that the absolute moduli obtained are of the order of  $5 \times 10^{11}$  dynes/cm<sup>2</sup> at nitrogen temperature. This compares favorably to  $3.5 \times 10^{11}$  dynes/cm<sup>2</sup> at room temperature computed from the elastic constants  $s_{11}$ ,  $s_{12}$ , and  $s_{44}$ , given by Zener<sup>(13)</sup> and Schmid and Boas<sup>(12)</sup> for copper at room temperature.

Figures 13 and 14 show the shear modulus as a function of



integrated electron flux. If only the coarse features of the curves are compared it is noted that both specimens exhibit an immediate rapid increase in G followed by a linear portion of slower increase. Overall increase in G was about 1.2% for specimen number one and 5% for specimen number two. If the initial steep increases are discounted, these are reduced to 0.9% and 3% respectively. Total integrated flux was about  $2.7 \times 10^{18}$  electrons/cm<sup>2</sup> for each. This flux was evaluated with respect to the area of the window and thus represents an upper limit. It is considered that the flux in the center of the beam at the specimen was approximately the same due to scattering in as well as out by the aluminum window. Specimen two was allowed to remain in a static condition at nitrogen temperature following the preliminary anneal and prior to any irradiation. Occasional measurements of  $\tau$  gave irregular variations between 463.5 and 467 for the quantity  $\frac{I_0}{\tau^2}$  until irradiation was commenced.

Other specimens were irradiated but the data was subsequently discarded due to doubt about exceeding critical stresses since they were made with a considerably heavier pendulum. Figure 15 (labeled "trial specimen") shows the irradiation phase for one of these. Although the data is in doubt it shows the same coarse features mentioned above. It is interesting to note also that all exhibit some sort of irregularity in the curve in the vicinity of  $1 \times 10^{18}$  electrons/cm<sup>2</sup>.

There is no immediate explanation for the apparent leveling off of specimen number one after  $1.5 \times 10^{18}$  electrons/cm<sup>2</sup>.



One other important change noted in a qualitative manner during the irradiation phase was the marked reduction in internal friction as evidenced by the decrease in damping of the torsional oscillations used to measure  $\tau$ . On specimen number two, in particular, readings were obtained with great difficulty and poor accuracy prior to irradiation due to the fact that the pendulum could hardly be made to swing 100 oscillations. Specifically, 100 oscillations left only 10% of the original amplitude. Immediately on commencement of irradiation the situation began to improve and after only  $2 \times 10^{17}$  electrons/cm<sup>2</sup> integrated flux, 35% of the original amplitude was left at the end of 100 oscillations. Finally, at the completion of the irradiation period with  $2.7 \times 10^{18}$  electrons/cm<sup>2</sup>, 85% amplitude remained following 100 swings.

Figures 16 and 17 show the "recovery" curves of specimens one and two with thermal annealing following irradiation. Neither specimen showed any tendency to return to pre-irradiation values and if anything the general trend was a slight continuing increase in shear modulus. For comparison, a control run was made with another specimen in which all conditions were identical except that the control specimen did not receive any irradiation. Instead it remained in a static condition for a comparable time prior to the annealing phase. A subsequent annealing procedure produced the graph in Figure 18 which is quite similar to those for the irradiated specimens.

In comparing specimens one and two it appears that specimen two gave larger changes and more erratic behavior in both





the irradiation phase and the anneal phase.



## CHAPTER VI

### DISCUSSION

Obviously there is insufficient data at this point to advance any new models for irradiation damage in metals. However previous proposals can be discussed in the light of these findings and further possibilities considered.

Any process conceivable as a mechanism for irradiation damage by electrons should, on the basis of the results of this investigation, explain the increase in shear modulus with irradiation, the decrease in internal friction, and non reversibility, or at least extreme stability with thermal annealing up to 400°C.

It is tempting to assign the cause of the increase in  $G$  with irradiation purely to the production of interstitial/vacancy pairs in confirmation of the predictions of Dienes. One would expect however, that if this were the case, subsequent annealing would at least show an eventual tendency to return toward the pre-irradiation value, as migration and recombination take place. In addition, calculations from best available data indicate that the increase noted in these specimens is several orders of magnitude greater than that predicted by Dienes. This conclusion is arrived at on the basis of theory and experiment. D. L. Dexter<sup>(2)</sup> has calculated that one atomic percent of interstitial/vacancy pairs should produce a change in resistivity in copper of  $10^{-6}$  ohm-cm independent of temperature. Meehan and Brinkman<sup>(9)</sup> have observed a linear change of  $4.2 \times 10^{-28}$  ohm-cm



per electron/cm<sup>2</sup> under experimental conditions nearly duplicating this investigation. Using these figures the atomic percent of interstitial-vacancy pairs created in specimens one and two by a total of  $2.7 \times 10^{18}$  electrons/cm<sup>2</sup> can be calculated to be about .001%. Figures 13 and 14 show an increase of up to 5% for this concentration whereas Dienes has predicted that an increase of 5% would require about 1% vacancy-interstitial pairs. Although these calculations at best probably only indicate order of magnitude, they do serve to show that much larger changes are taking place than those predicted due only to the presence of interstitial-vacancy pairs.

Thus, since no tendency to recover was displayed by any specimen and in view of the generally large increase with a rather moderate total flux, it is felt that some process was occurring along with the production of point defects, which not only increased the shear modulus itself but also led to the incorporation of the point defects into a rather stable configuration.

The most promising possibilities seem to lie in the consideration of dislocation theory in connection with the techniques used in this investigation to measure shear modulus. An isotropic homogeneous crystal with no dislocations would most certainly have a larger shear modulus than is actually observed in imperfect crystals. The presence of dislocations furnishes a means of distortion with a much smaller applied stress due to the glide of the dislocations. As stress is applied to a crystal, a dislocation line, representing the edge of an incomplete



plane of atoms, can glide along the slip plane having only to overcome the resistive force due to a single jump from one atomic plane to the next. Without the dislocation, the whole crystal must be deformed requiring considerably greater stress.

If a section of a dislocation is pinned at each end by say a point defect or jog (considerably more resistant to motion along the slip plane perpendicular to the dislocation) the dislocation is still partially effective in facilitating strain. An applied stress will cause the dislocation to bow out from its pinning points as the center portion continues to glide while the ends stay fixed. Conversely however, any process which pins already present dislocations more frequently along their length, should lead to an increased shear modulus as the dislocations would be becoming less effective as agents for facilitating strain.

Assuming a certain density of dislocations present in the specimen depending on its past treatment, the stresses introduced by the oscillations of the pendulum should cause these dislocations to glide back and forth and their stress fields to sweep through a certain volume of the crystal in the process. The point defects created by irradiation could be picked up by these dislocations and act to relieve the stress fields, thus becoming stable notches in the line defects. The pinning effect of the interstitials and vacancies (now notches) on the dislocations would thus furnish an explanation of both the increased shear modulus and decreased internal friction, since the motion of dislocations is certainly an energy dissipative process.





Since the increase in  $G$  would be a function not only of irradiation but also of dislocation density, a possible explanation would also be provided for the difference in behavior of specimens one and two.

If a dislocation in a crystal were sufficiently pinned, its mobility with applied stress could be reduced to the point that its presence no longer affected the shear modulus. If thermal annealing were to remove such a dislocation, its loss would not be detectable by methods of this experiment. Further, the processes proposed by many involving the migration of point defects are certainly not to be discounted for it is entirely possible that these effects could be obscured if immobilization of dislocations is taking place.



## CHAPTER VII

### CONCLUSIONS

Irradiation of pure copper with two Mev electrons results in a large increase in shear modulus and a decrease in internal friction. The mechanism involved appears to be concerned with the production of very stable configurations of defects which do not anneal out up to 400°C.

Obviously there still remain many possibilities which might account for the phenomenon observed. All specimens had a certain amount of oxide coating which could conceivably have contributed one way or another to change, not only through reduction of the oxide by the electron beam but also through some sort of accumulation of dislocations at the boundary between the oxide and the metal. It is further conceivable that some sort of impurities could have been driven into the copper from the surrounding medium.

The systematic elimination of these possibilities should form the starting point for continued research. The most fruitful avenue of further investigation seems to lie in a consideration of the interaction of dislocations with the interstitial-vacancy pairs presumed to be the primary agents of damage. A study similar to this using specimens containing varied amounts of cold work would be extremely valuable in supplying a correlation between density of dislocations and radiation effects.



## BIBLIOGRAPHY

1. Cooper, E.P. and M. M. Mills                      U. S. REPORT AECD-3796, 11p (1950)
2. Dexter, D.L.                      PHYS. REV. 87, 768 (1952)
3. Dieckamp, H. and Crittenden, E.C. Jr.                      PHYS. REV. 94, 1418 (1954)
4. Dieckamp, H.                      PHYS. REV. 98, 1531 (1955)
5. Dienes, G.J.                      PHYS. REV. 86, 228 and PHYS. REV. 87, 666
6. Eggen and Laubenstein                      PHYS. REV. 91, 238
7. Glenn, J.W.                      ADVANCES IN PHYSICS (a quarterly supplement of the Philosophical Magazine) Vol. 4, Number 16, October 1955, Taylor and Francis Ltd, London, page 381.
8.                      HANDBOOK OF CHEMISTRY AND PHYSICS, 36th Ed., 1954-55, Chemical Rubber Publishing Co., page 2371.
9. Meechan, C.J. and Brinkman, J.A.                      AN ELECTRICAL RESISTIVITY STUDY OF LATTICE DEFECTS introduced in copper by 1.25 Mev electron irradiation at 80°K, Atomics International (Div. of N.A.A.), Canoga Park, Calif.
10. Schmid, E. and Boas, I.W.                      PLASTICITY OF CRYSTALS, F.A. Hughes and Co., Ltd, London, 1950, page 21.
11.                      Ibid, page 113
12.                      Ibid, page 191
13. Zener, C.                      ELASTICITY AND ANELASTICITY OF METALS, University of Chicago Press, Chicago, 1948, page 17.



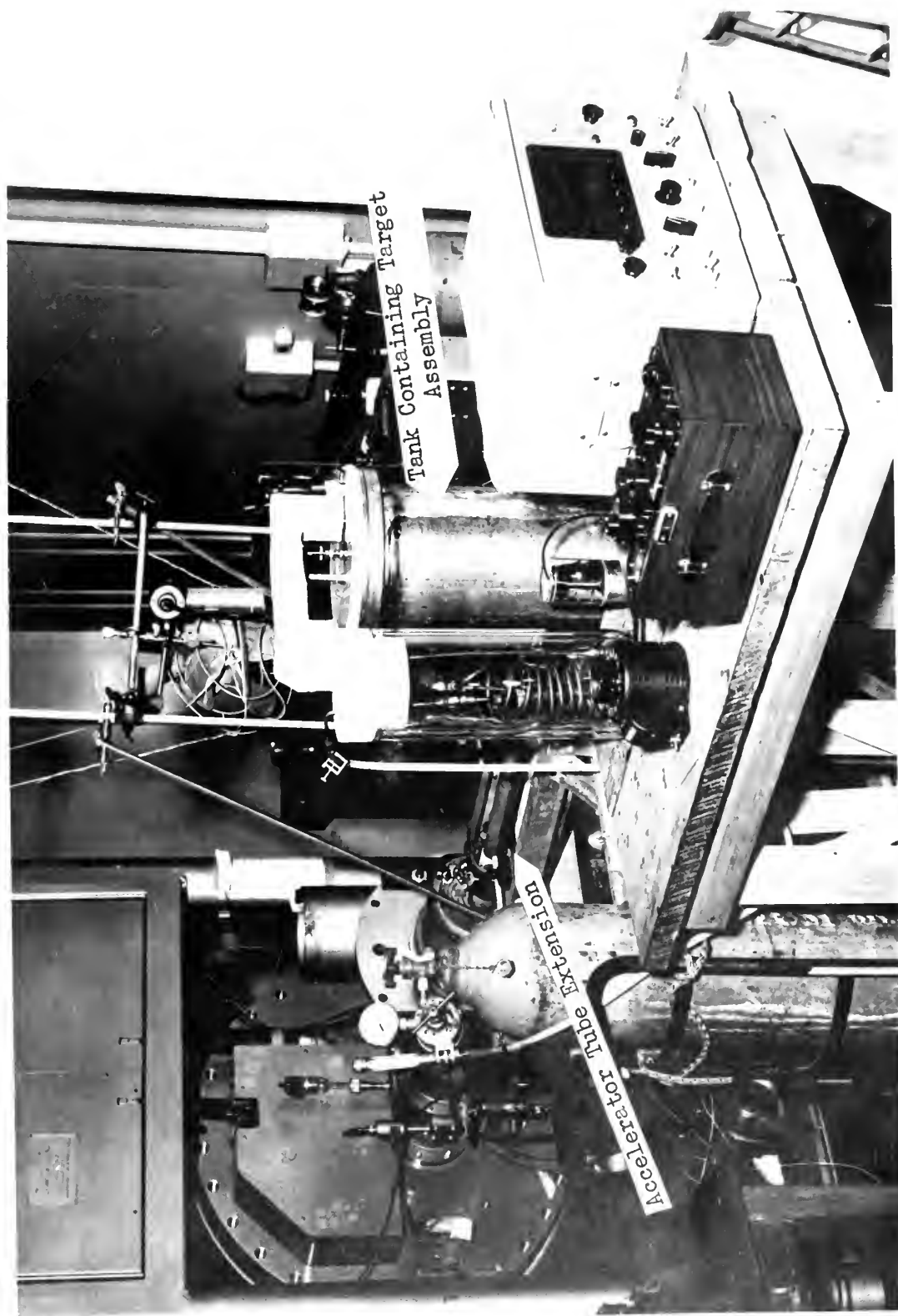


FIG. 1

GENERAL ARRANGEMENT OF EQUIPMENT





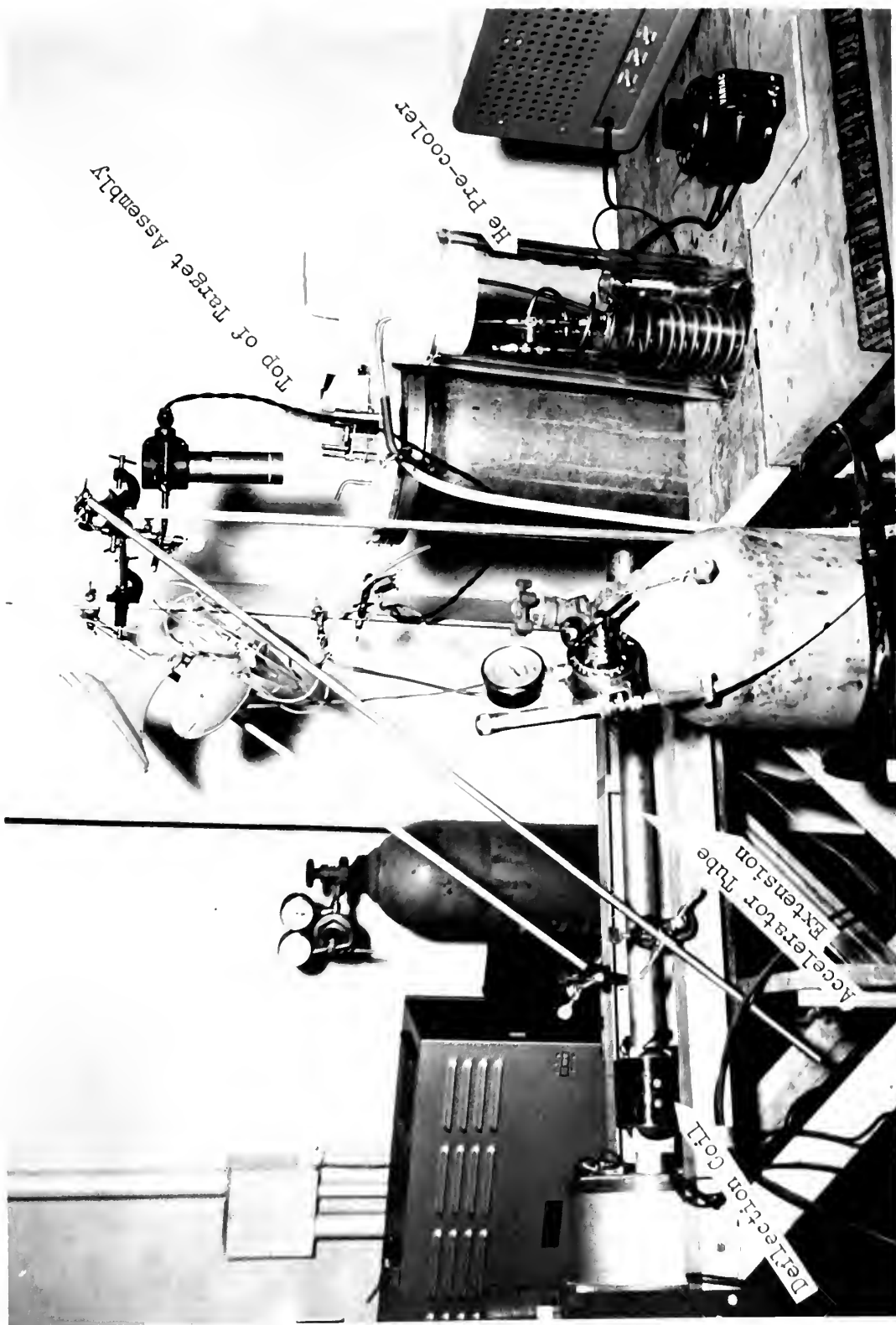


FIG. 2

DEFLECTION, TARGET AND COOLING SYSTEM



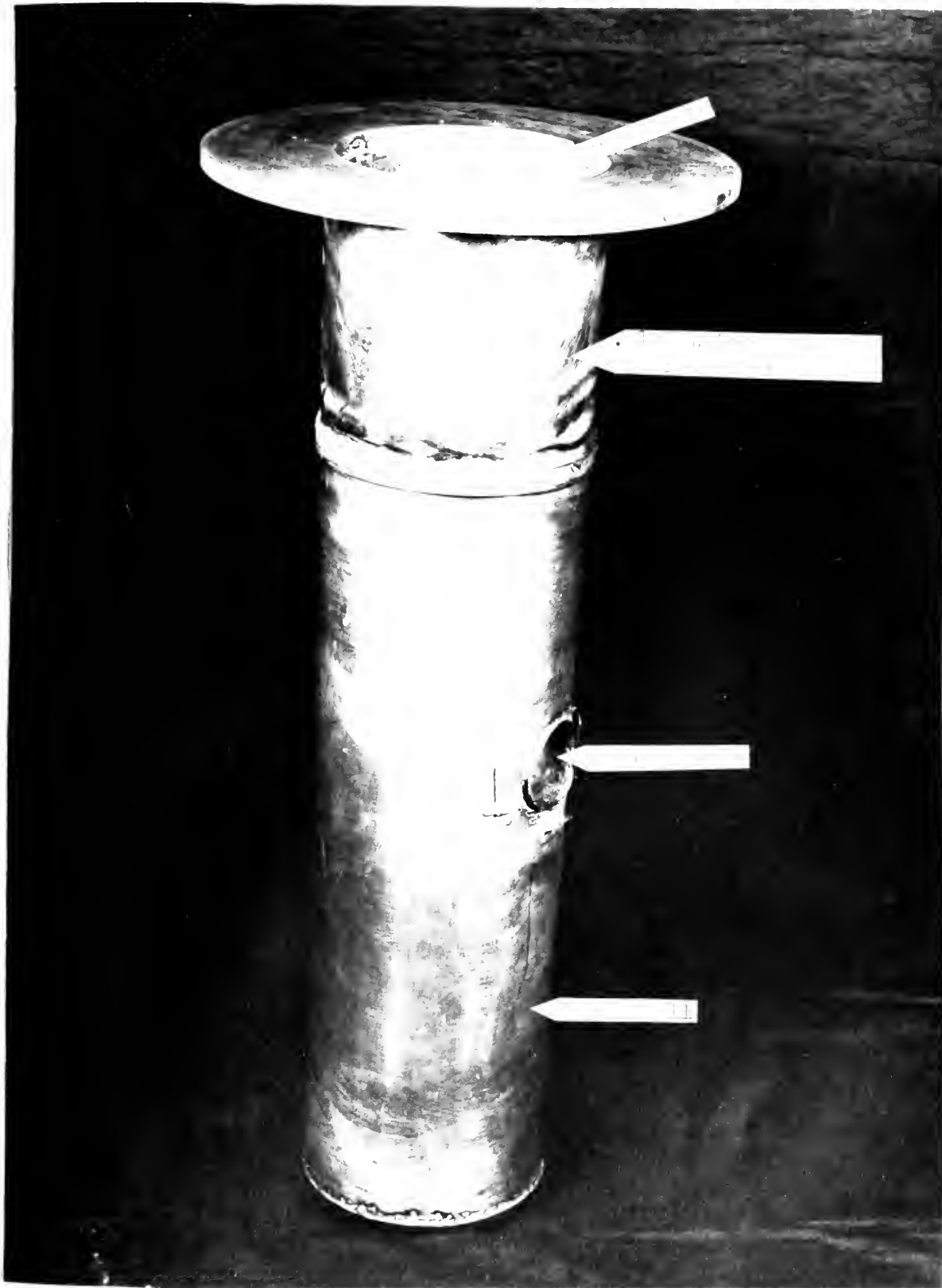


FIG. 1

"VACUUM" 1 "







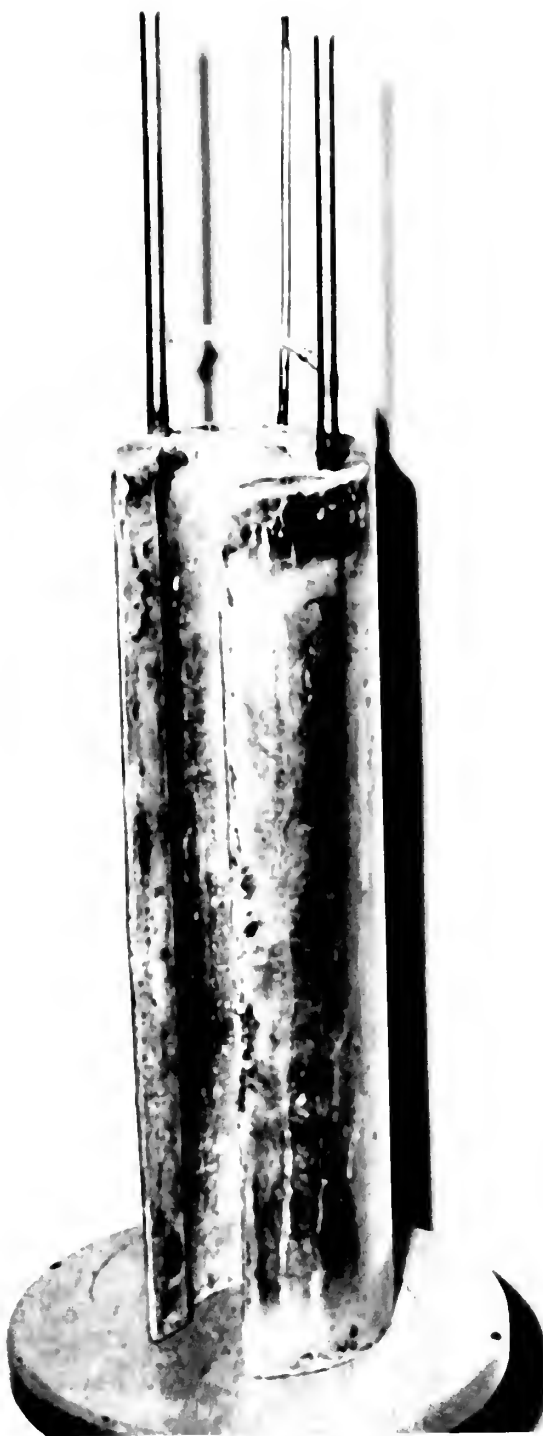


FIG. 5

LIQUID NITROGEN RESERVOIR





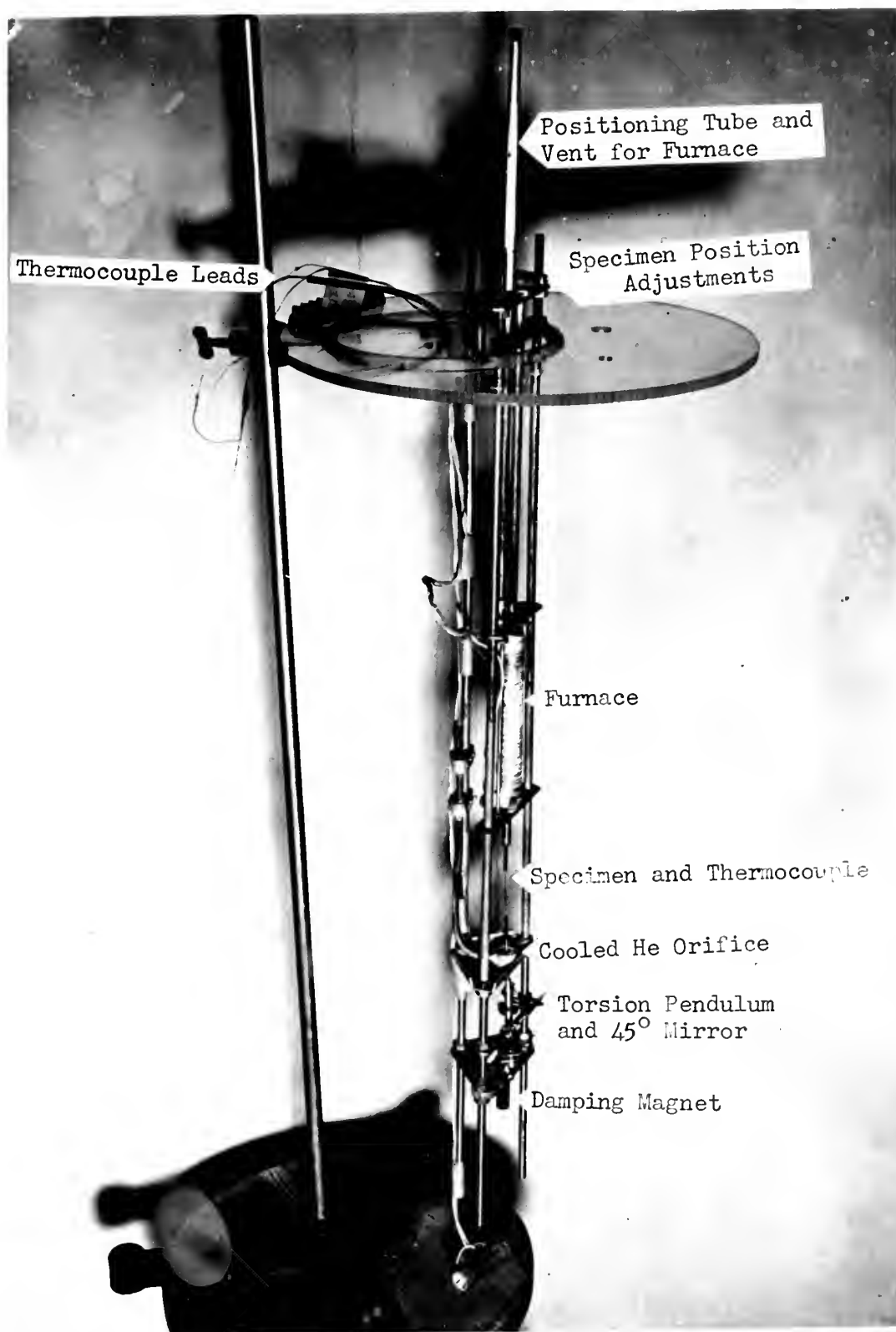


FIG. 6

TARGET ASSEMBLY



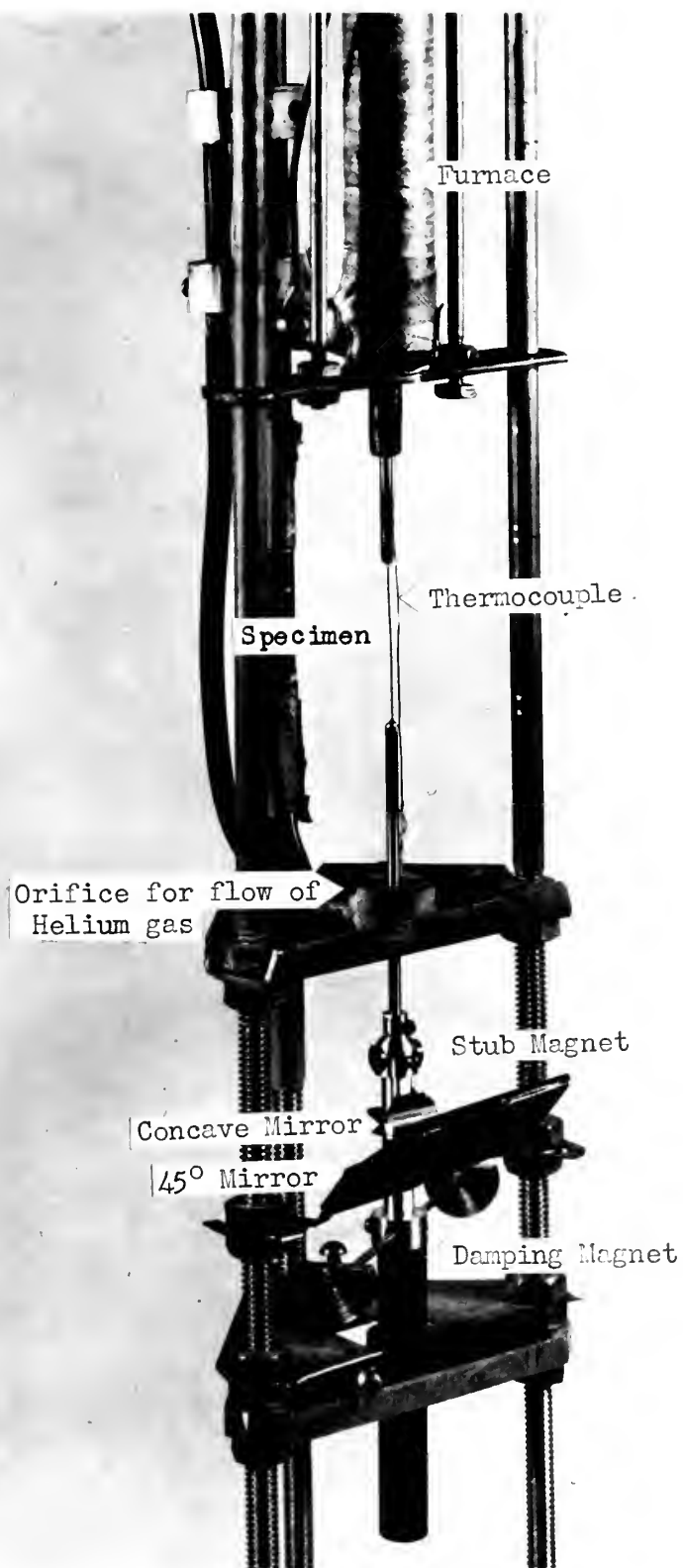


FIG. 7

LOWER PORTION OF TARGET ASSEMBLY





FIG. 8

HEATER IN LOWERED POSITION  
FOR PULSE ANNEALS OF SPECIMEN



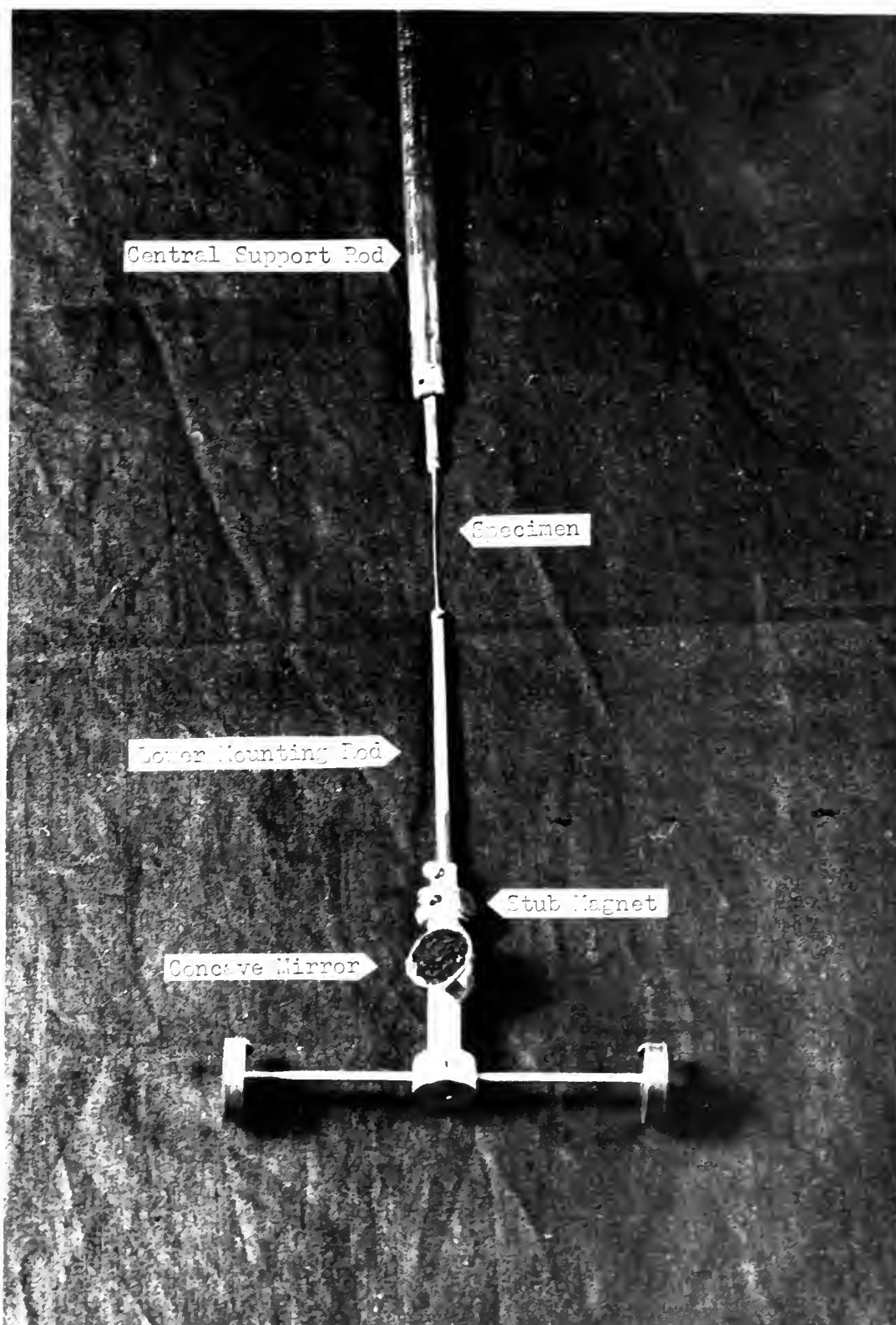


FIG. 9  
TORSION PENDULUM





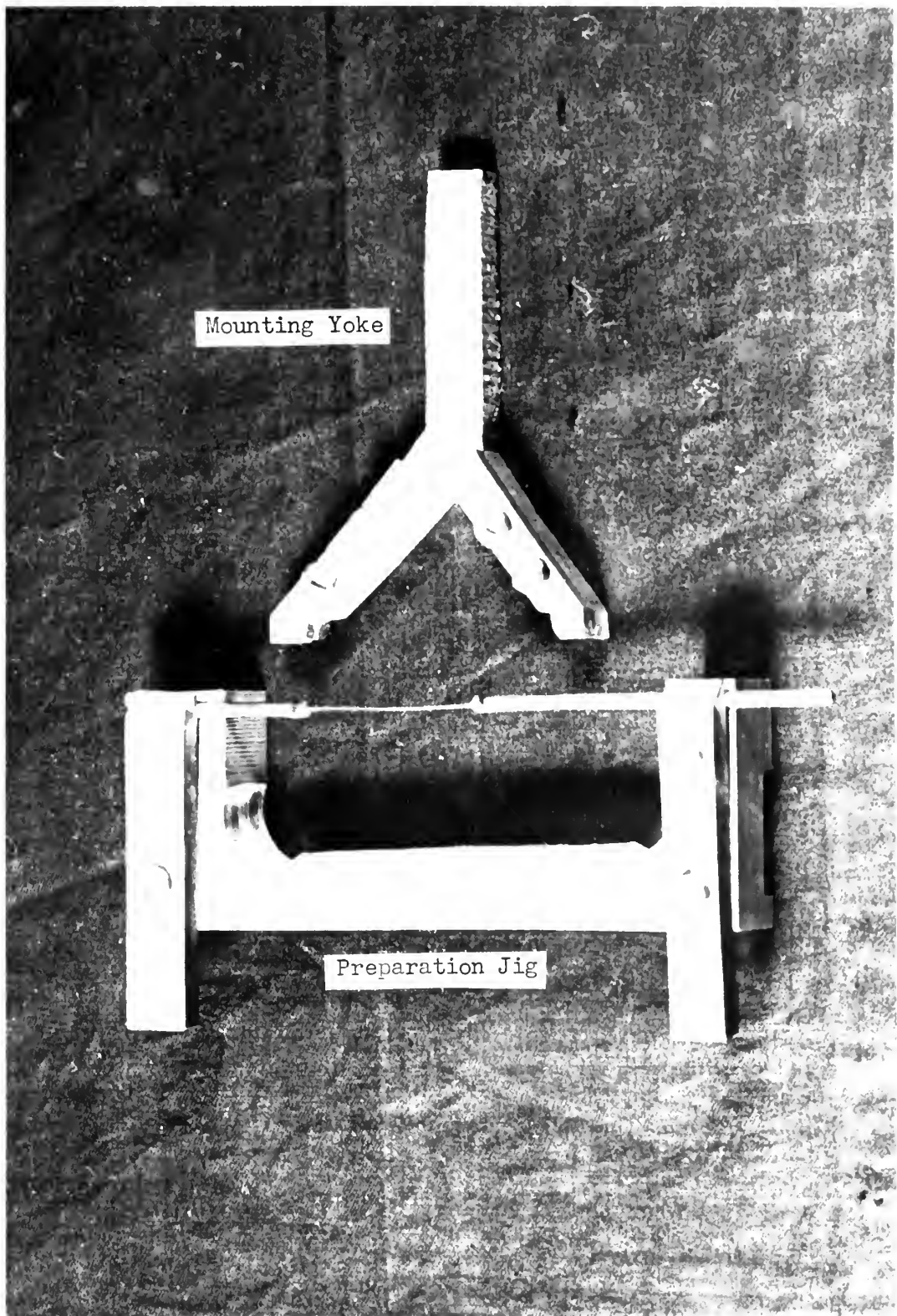


FIG. 10

PREPARATION AND HANDLING EQUIPMENT FOR SPECIMEN





(a)

Coverage of Window



(b)

Exposure of Specimen  
and Thermocouple to  
electron flux

FIG. 11

OZALIDS OF WINDOW AND SPECIMEN EXPOSED BY ELECTRON BEAM



INNER AND OUTER VACUUM TANKS

DEFLECTION

COIL

DRIFT TUBE

TARGET SPACE

570V

60~

$\mu A$

ARRANGEMENT OF A GRID AND PLATE, TEMPORARILY INSTALLED, TO OBTAIN CURVE, WITH VACUUM EXTENDED TO TARGET SPACE.

NOTE: CURVE DRAWN FOR 2 MEV ELECTRONS AND 130  $\mu$ -AMP BEAM CURRENT. MEASURED IN VACUUM.

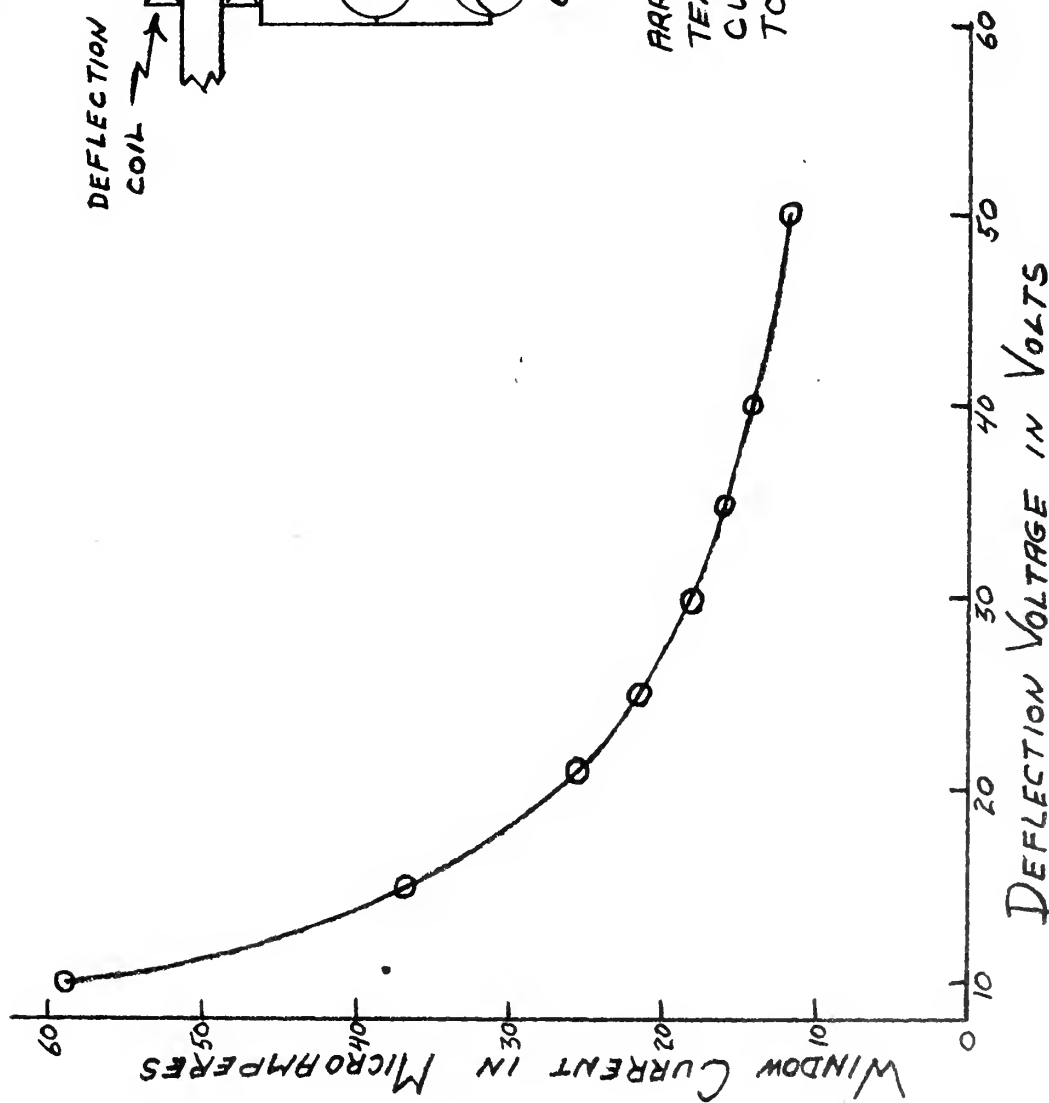


FIG. 12  
CURRENT THROUGH WINDOW  
vs  
DEFLECTION VOLTAGE



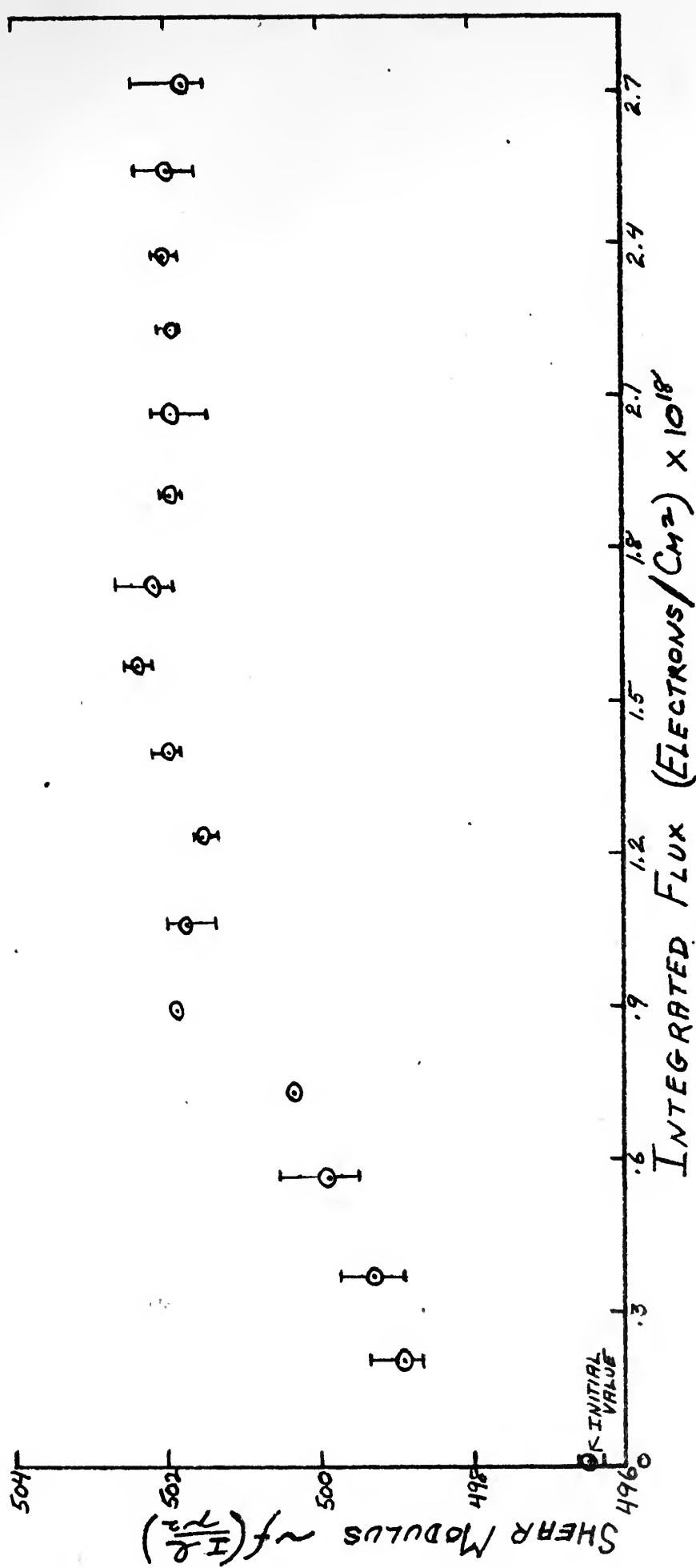
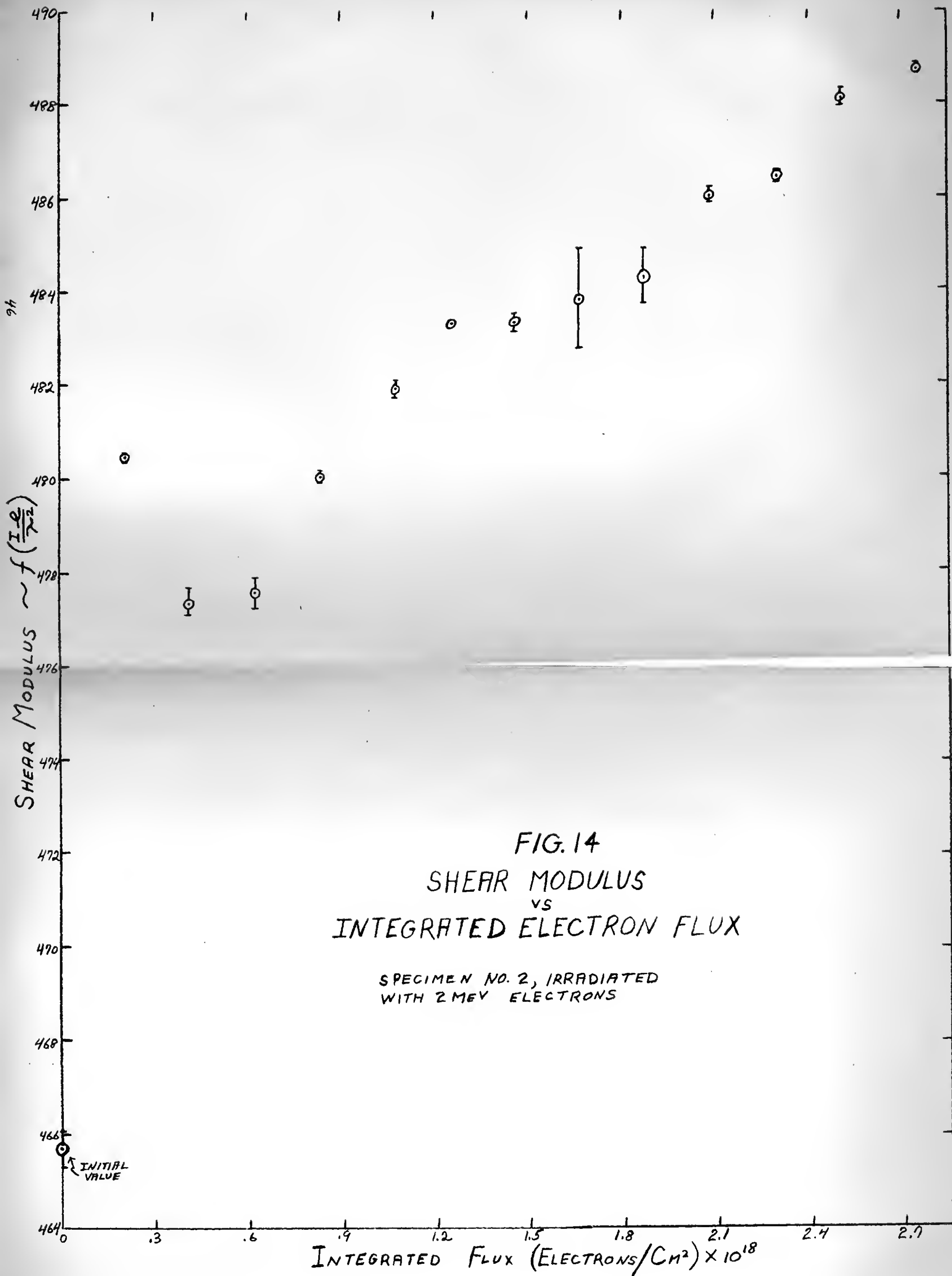


FIG. 13  
SHEAR MODULUS  
VS  
INTEGRATED ELECTRON FLUX

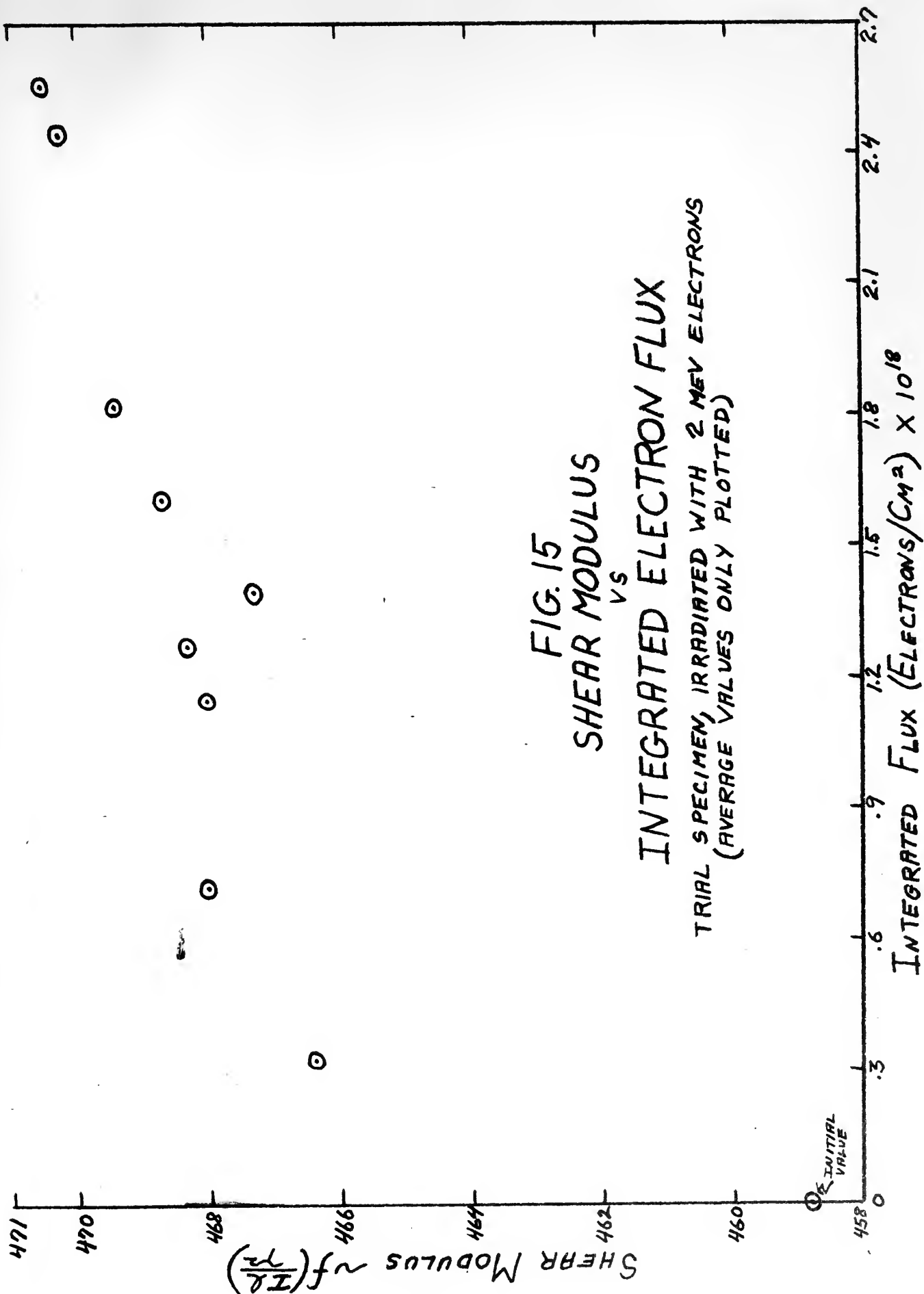
SPECIMEN NO. 1, IRRADIATED WITH 2 MEV ELECTRONS



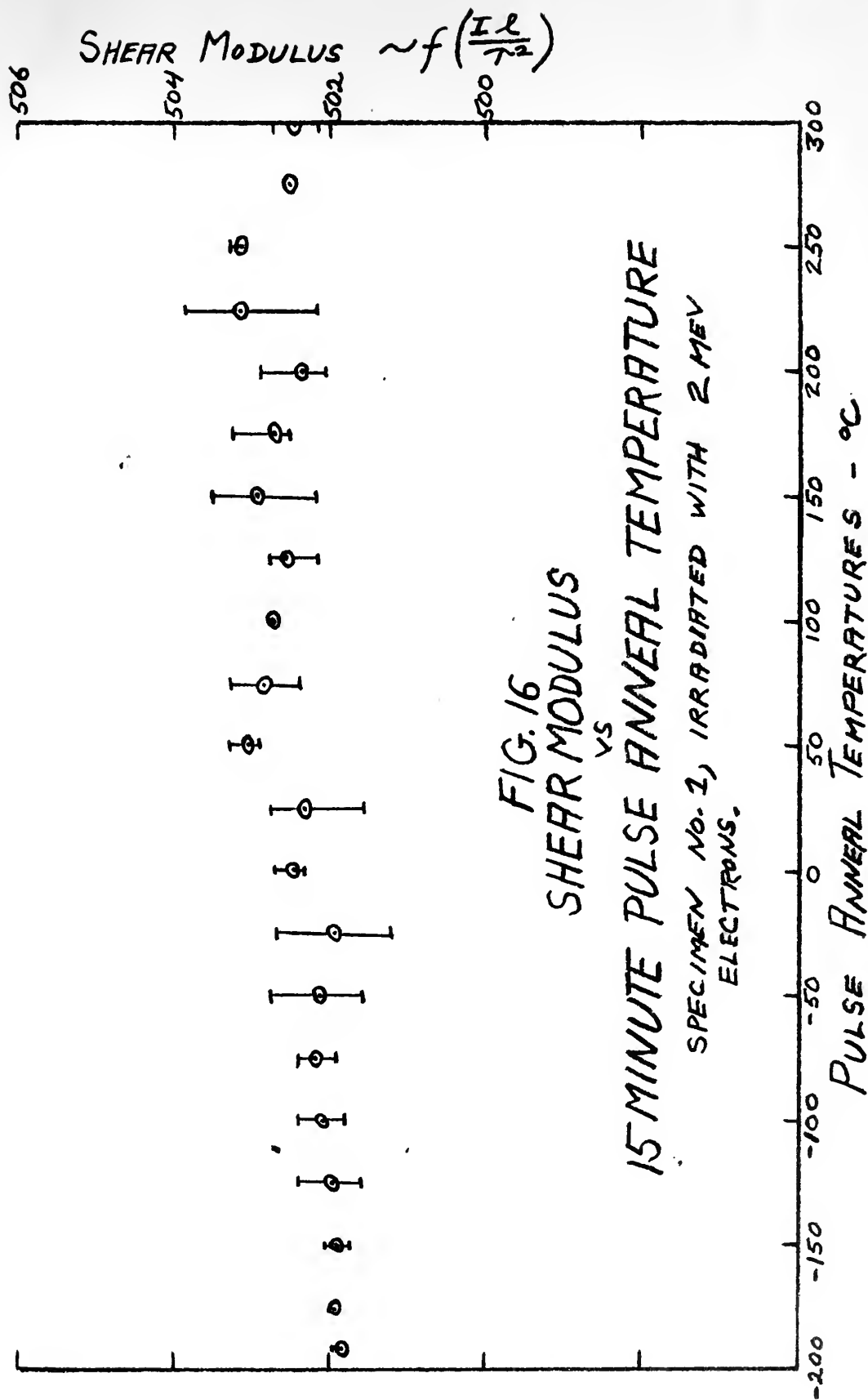














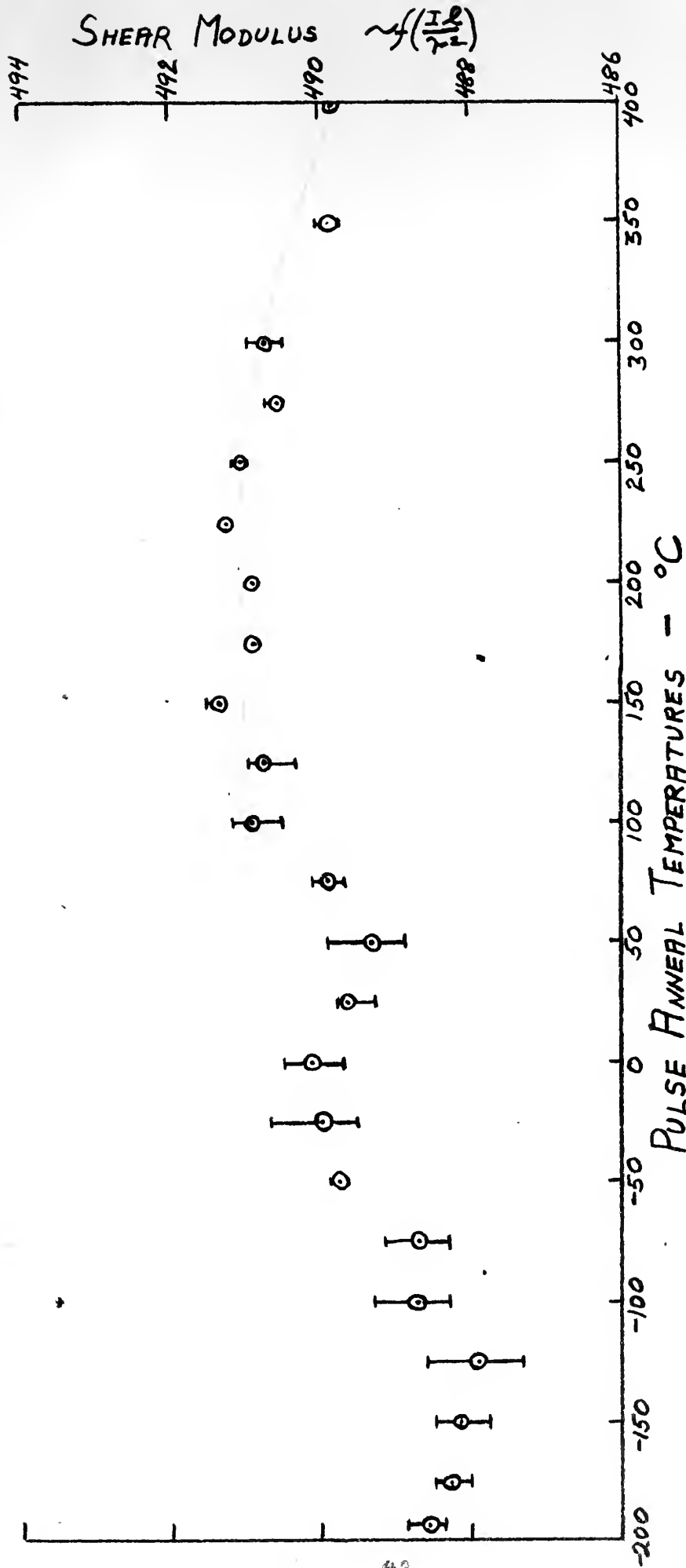


FIG. 17  
SHEAR MODULUS  
vs  
15 MINUTE PULSE ANNEAL TEMPERATURES  
SPECIMEN NO. 2, IRRADIATED WITH 2 MEV ELECTRONS.





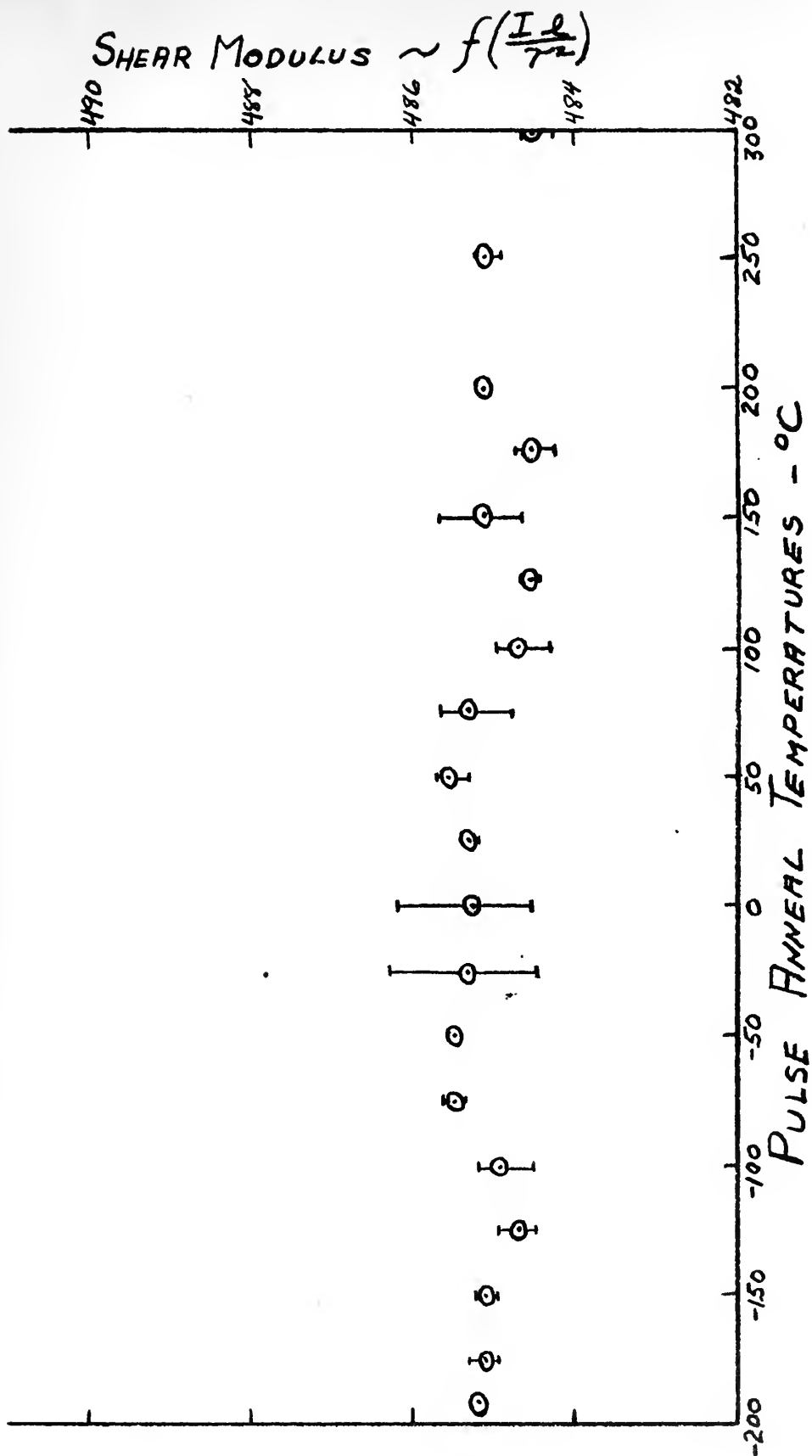


FIG. 18  
15 MINUTE PULSE ANNEALS OF  
UNDAMAGED SPECIMEN  
CONTROL RUN











OC 24 57  
DE 9 58  
DE 23 58

4995

800

INTERLIB  
SR1-Mexico

Thesis  
P753

Powell

23011

The effects of electron  
damage on the shear modulus  
of copper.

OC 24 57

4995

DE 9 58

800

DE 23 58

INTERLIB

~~SR1-Mexico~~  
SR1-Mexico Post US

P753 Powell

23011

The effects of electron damage  
on the shear modulus of copper.

thesis P753

The effects of electron damage on the sh



3 2768 001 92362 6  
DUDLEY KNOX LIBRARY